

MELDOLA MEDAL LECTURES*

I Molecular Shapes

By J. K. Burdett†

DEPARTMENT OF INORGANIC CHEMISTRY, THE UNIVERSITY OF
NEWCASTLE UPON TYNE, NEWCASTLE UPON TYNE, NE1 7RU

1 Introduction

For many years chemists have explored structural aspects of simple main group compounds guided by several simple theoretical tools that have proved invaluable. The Valence Shell Electron Pair Repulsion (VSEPR) model, devised by Sidgwick and Powell and consolidated by Nyholm and Gillespie, is a qualitative predictor of the angular geometry of an AH_n or AX_n system with a main group (A) central atom.¹ The ideas of Walsh,² published twenty-five years ago, provided a simple molecular orbital rationale of these structures and, in addition, were able to predict the geometries of excited states which VSEPR could not do. One interesting feature of the two methods is that whereas the VSEPR scheme emphasizes electron-electron interactions, and ignores central-atom-ligand interactions, the opposite is true for Walsh's molecular orbital approach, which is just concerned with the changing magnitudes of central atom orbital-ligand orbital overlap on distortion. A linking piece in this structural jigsaw was provided by Bartell's adaptation³ of the second-order (or pseudo) Jahn-Teller effect to structural main group chemistry. Shortly afterwards Pearson published⁴ his symmetry rules for the prediction of molecular geometry, which included and extended Bartell's work. We shall find, however, that these well proven methods for looking at main group structures need to be replaced when rationalizing the shapes of transition-metal complexes. Steric effects are often very important in influencing reactions and structures. Recently Glidewell⁵ has widely applied the 'hard sphere' ideas of Bartell⁶ to this area and the interplay of steric and electronic controls on geometry is one that we shall return to. Many sets of quantitative molecular orbital calculations have been performed at varying levels of sophistication in efforts to calculate bond angles. It is, however, the purpose of this

*These lectures were delivered in April 1978 at the Annual Chemical Congress, University of Liverpool.

†Present address: Chemistry Department, University of Chicago, 5735 South Ellis Avenue, Chicago, Illinois 60637, U.S.A.

¹ R. J. Gillespie, 'Molecular Geometry', Van Nostrand-Rheinhold, London, 1972.

² A. D. Walsh, *J. Chem. Soc.*, 1953, 2260, and following papers.

³ L. S. Bartell, *J. Chem. Educ.*, 1968, **45**, 754.

⁴ R. G. Pearson, *J. Amer. Chem. Soc.*, 1969, **91**, 1252, 4947.

⁵ C. Glidewell, *Inorg. Chim. Acta*, 1975, **12**, 219; 1976, **20**, 113.

⁶ L. S. Bartell, *J. Chem. Phys.*, 1960, **32**, 827.

lecture to review methods which lead to an *understanding* of molecular shapes at a basic level. One may recall that in Hoffmann's view '... to understand an observable means being able to predict albeit qualitatively the result that a perfectly reliable calculation would yield for that observable'.⁷

2 Shapes of Main Group Molecules

VSEPR and Walsh's Scheme.—The angular geometries of simple main group molecules are well matched by the predictions of the theoretical tools we have just mentioned. (The exceptions are of interest in themselves.) For the AH_3 and AX_3 molecules ($A = B, C, N$; $X = \text{halogen } \textit{etc.}$) the VSEPR method correctly predicts BH_3 to be trigonal planar (three pairs of electrons) and NH_3 to be pyramidal (four pairs of electrons). The number of electrons which we use in the VSEPR count is all the valence ($ns + np$) electrons on the central atom plus (usually) one from each of the ligands. Where double bonding is possible between A and X (*e.g.* $X = O$) only the electron from the σ part of the interaction is included. In some cases two electrons come from each of the ligands. Thus $C(PR_3)_2$ contains two filled shell ligands (PR_3) which contribute two electrons to the VSEPR count. With the four carbon valence electrons, a total of four electron pairs are included in the scheme, which rationalizes the non-linear structure⁸ of the molecule (isoelectronic with OF_2). The methyl group with three and a half pairs provides a problem since how does half an electron pair behave? The Walsh diagram for the AH_3 system is shown in Figure 1. (For AX_3 the situation is similar.) It shows how the valence orbitals of the unit qualitatively change in energy as the molecule distorts. Walsh arrived at the angular dependence of the orbital energies simply by considering in qualitative terms how the ligand–central atom overlap integrals changed on distortion. (This may be put on a semi-quantitative basis by applying to the main group case⁹ the ideas we describe below for transition-metal systems.) Parr has shown¹⁰ how valence bond methods arrive at similar results. For BH_3 with two electrons in the $1a'_1$ and four in the $1e'$ orbital bending is obviously unfavourable. For NH_3 with two electrons in $1a''_2$ an overall stabilization on bending is possible. With only one electron in this orbital (CH_3), is the stabilization energy afforded this electron on bending sufficient to overcome the opposing effect of the lower energy electrons? Jordan and Longuet-Higgins¹¹ suggested that the radical would be planar, whereas Linnett and Poë¹² suggested that it would be pyramidal. In fact the result of gas phase electronic spectral studies¹³ and e.s.r. results¹⁴ on matrix

⁷ R. Hoffmann, *Accounts Chem. Res.*, 1971, 4, 1.

⁸ A. T. Vincent and P. J. Wheatley, *J.C.S. Dalton*, 1972, 617.

⁹ J. K. Burdett, *Structure and Bonding*, 1976, 31, 67.

¹⁰ G. W. Schnuelle and R. G. Parr, *J. Amer. Chem. Soc.*, 1972, 94, 8974.

¹¹ P. C. H. Jordan and H. C. Longuet-Higgins, *Mol. Phys.*, 1962, 5, 121.

¹² J. W. Linnett and A. J. Poë, *Trans. Faraday Soc.*, 1951, 47, 1033.

¹³ G. Herzberg, *Proc. Roy. Soc.*, 1961, A262, 291.

¹⁴ R. W. Fessenden and R. H. Schuler, *J. Chem. Phys.*, 1963, 39, 2147.

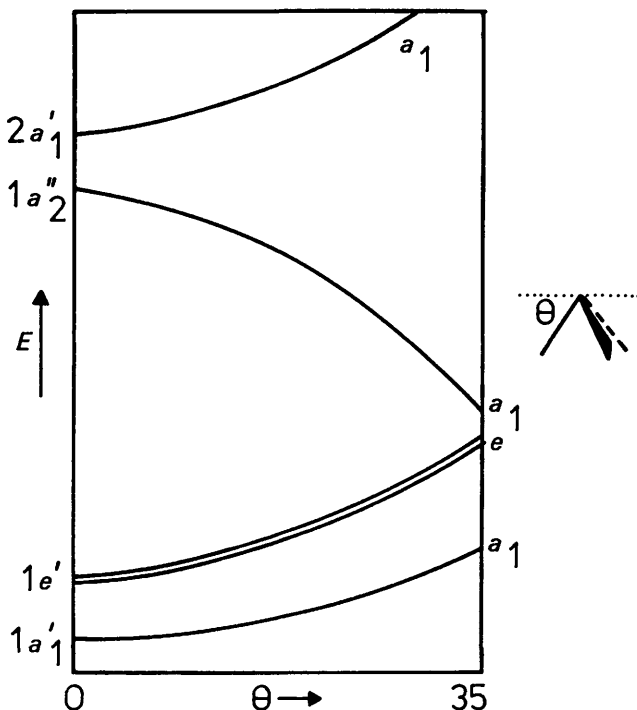


Figure 1 Walsh diagram for an AH_3 molecule within the C_{3v} distortion co-ordinate

isolated CH_3 suggest that it is, or is very close to being, planar; the second row analogue SiH_3 , however, is pyramidal.¹⁵ Matrix studies^{14,16,17} also show that substituted methyl radicals are pyramidal (*e.g.* CF_3 , CHF_3 , CCl_3). Thus on the VSEPR model three and a half electron pairs behave differently according to the substituents attached to the main group atom. But the vibrational data on matrix isolated CH_3 are intrinsically very interesting. The radical was made initially in two ways [reactions (1)¹⁸ and (2)¹⁹].



When made by reaction (1) the out-of-plane bending mode (ν_2) of the radical at 611 cm^{-1} was associated with an unusual ratio of $\nu_2(H)/\nu_2(D)$ (Table 1). This could be rationalized either by a bond angle smaller than that in NH_3 in its

¹⁵ R. L. Morehouse, J. J. Christiansen, and W. Gordy, *J. Chem. Phys.*, 1966, **45**, 1751.

¹⁶ R. W. Fessenden and R. H. Schuler, *J. Chem. Phys.*, 1965, **43**, 2704.

¹⁷ L. Andrews, *J. Chem. Phys.*, 1968, **48**, 972; *J. Phys. Chem.*, 1967, **71**, 2761.

¹⁸ D. E. Milligan and M. E. Jacox, *J. Chem. Phys.*, 1967, **47**, 5146.

¹⁹ L. Andrews and G. C. Pimentel, *J. Chem. Phys.*, 1967, **47**, 3637.

Table 1 Vibrational data for CH₃ and perturbed CH₃ radicals

	ν_2 cm ⁻¹	$\nu(\text{H})/\nu(\text{D})^a$	
CH ₃ ··· LiBr	730	1.288	normal positive anharmonicity
CH ₃ ··· LiI	730		
CH ₃ ··· NaBr	700		
CH ₃ ··· NaI	696	1.305	
CH ₃ ··· KI	680		negative anharmonicity
CH ₃	611	1.319	

^a1.291 for harmonic oscillator

electronic ground state (which is unlikely) or by a large negative anharmonicity of a planar structure. This type of anharmonicity is well documented for a small number of systems. (Amongst these is the out-of-plane bending mode of the first excited state of NH₃ [(1e')⁴(1a'')¹(2a')¹], which is also planar²⁰ and closely related to the present problem.) Intriguingly the radical formed in reaction (2) (MX = LiI) showed a higher value of ν_2 and a small (normal) positive anharmonicity (Table 1). In order to understand this behaviour we need to look at the third approach to molecular geometry.

CH₃ and the Second-order Jahn-Teller Effect.—The strategy of this method uses the perturbation expansion of the energy of a molecule^{3,4,21–23} on distortion along a co-ordinate, Q_i . If we write the perturbed Hamiltonian as equation (3)

$$\begin{aligned} \mathcal{H}' &= \mathcal{H} + \left(\frac{\partial \mathcal{H}}{\partial Q_i}\right)_0 Q_i + \frac{1}{2} \left(\frac{\partial^2 \mathcal{H}}{\partial Q_i^2}\right) Q_i^2 + \dots \\ &= \mathcal{H} + \mathcal{H}'_i Q_i + \frac{1}{2} \mathcal{H}''_{ii} Q_i^2 + \dots \end{aligned} \quad (3)$$

then from first- and second-order perturbation theory for the electronic ground state ($|0\rangle$)

$$E' - E = \langle 0 | \mathcal{H}'_i | 0 \rangle Q_i + \frac{1}{2} Q_i^2 \left[\langle 0 | \mathcal{H}''_{ii} | 0 \rangle - 2 \sum_j' \frac{|\langle 0 | \mathcal{H}'_{ij} | j \rangle|^2}{\Delta \epsilon_{0j}} \right] \quad (4)$$

The first term in this energy series is the first-order Jahn-Teller term.²⁴ It will be non-zero for (i) any electronic state if \mathcal{H}'_i is associated with a totally symmetric mode, and (ii) an orbitally degenerate electronic state if \mathcal{H}'_i is associated with a mode which reduces the molecular symmetry. We usually ignore (i) and focus on the predictions for degenerate electronic states where the distortion

²⁰ A. D. Walsh and P. A. Warsop, *Trans. Faraday Soc.*, 1961, **57**, 345.

²¹ R. F. W. Bader, *Mol. Phys.*, 1960, **3**, 137.

²² H. C. Longuet-Higgins, *Proc. Roy. Soc.*, 1956, **A235**, 537.

²³ J. K. Burdett, *Appl. Spec. Rev.*, 1970, **4**, 43.

²⁴ H. A. Jahn and E. Teller, *Proc. Roy. Soc.*, 1937, **A161**, 220.

removes this degeneracy. A tabulation of the permitted distortions Q_i for given geometries and electronic state is given by Jotham and Kettle.²⁵

The second term (of order Q_i^2) in equation (4) is the one which will mainly concern us here and represents the force constant associated with the distortion.

It consists of two parts, a 'classical' force constant, $\left\langle \frac{\partial^2 V}{\partial Q_i^2} \right\rangle$, and a relaxation part—describing how the electronic charge distribution changes or relaxes so as to reduce the overall force constant. If the summation is truncated at the first excited state $|n\rangle$ then the force constant is given by equation (5). If there is a small $\Delta\epsilon$ [control-

$$k_0 = \langle 0 | \mathcal{H}_{ii} | 0 \rangle - 2 \frac{|\langle 0 | \mathcal{H}_{i1} | n \rangle|^2}{\Delta\epsilon} \quad (5)$$

led by the size of the highest occupied molecular orbital (HOMO)—lowest unoccupied molecular orbital (LUMO) separation] then the relaxation term may be large and overwhelm the classical force constant. The resulting negative force constant implies that the molecule will spontaneously deform away from that geometry along the co-ordinate Q_i , the actual choice of which is regulated simply by the symmetry properties of the ground and first excited electronic states.

An alternative approach is the following. We need to find that distortion co-ordinate which will result in the HOMO and LUMO having identical symmetry properties (*i.e.* belong to the same symmetry species in the distorted molecule). As this distortion progresses the HOMO and LUMO will heavily mix together and the two energy levels will 'repel' one another. The lower energy component (HOMO) which contains one or two electrons will be stabilized by such an interaction as shown in Figure 2. If the dynamics of the system are controlled by the energetic behaviour of the HOMO, then the molecule as a whole will be stabilized by such a distortion.

From group theory we can determine the symmetry of Q_i such that the integrand $|\langle 0 | \mathcal{H}_{i1} | n \rangle|^2$ may be non-zero. We may express the numerator in terms of the transition density $\phi_0^* \phi_n$, where ϕ_0 is the orbital in the ground state and ϕ_n is the orbital in the excited state which hold the 'excited' electron. Figure 3(a) shows schematically how the symmetry species of Q_i is determined for AH_3 molecules ($A = B$ or N) and also for ClF_3 . The direct product of the symmetry species of ϕ_0 and ϕ_n must contain either a''_2 or e' for the molecule to distort, as shown in Figure 3(b). Hence the planar structure of BH_3 , pyramidal structure of NH_3 , and T-shape of ClF_3 are neatly rationalized. (It may be noted here that the latter geometry was one not mentioned by Walsh.) The same method can be used to reproduce the geometries of CF_4 , SF_4 , XeF_4 etc., and usually similar predictions to those from VSEPR are obtained. However, this method does require that we have a knowledge of the MO structure of the symmetric geometry before we can begin. Note that in Figure 3(a) it is the lowest energy 'transition' which determines the geometry. A higher energy transition ($1e' \rightarrow 2a'_1$) would give rise to a transition density (and Q_i) of species e' for BH_3 , which in practice does not give rise to any static distortion. A manifestation of this contribution does however

²⁵ R. W. Jotham and S. F. A. Kettle, *Inorg. Chim. Acta*, 1971, 5, 183.

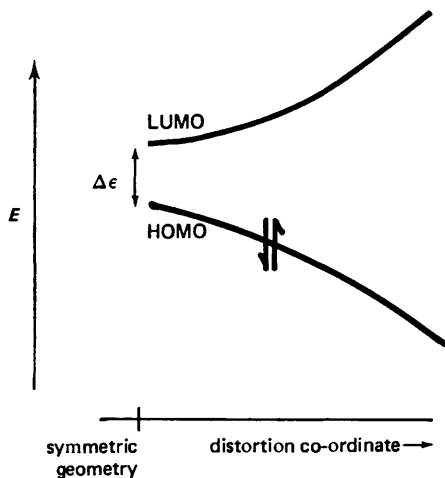


Figure 2 The stabilization of the HOMO brought about by the distortion co-ordinate which causes the HOMO and LUMO to have identical symmetry properties

turn up in the vibrational force field of the planar molecule.²¹ The stretching bond-bond interaction force constant is positive, which shows that the relaxation term of equation (4) is not zero but not large enough to overcome the classical constant.

The result of variation of ligand electronegativity can be seen by its effect on the size of the energy gap $\Delta\epsilon$. For the NX_3 case this will be largely set by the energy difference between $1a''_2$ and $2a'_1$. The $1a''_2$ orbital remains approximately unchanged in energy but the orbitals involved in σ interactions (e.g. $2a'_1$) drop in energy and $\Delta\epsilon$ becomes smaller. The driving force away from planar for NX_3 species should then be larger as X becomes more electronegative. An alternative way of looking at the increasing tendency for AX_3 molecules to pyramidalize as the electronegativity of the X ligands increase is provided²⁶ by the theory of isovalent hybridization.²⁷ Briefly, the more electronegative the ligand X the more polarized the AX bond. In MO language this means that the AX bond will contain more A atom p -character. Increasing central atom p -character in a hybrid leads to smaller X—A—X angles (recall sp , 180° ; sp^2 , 120° ; sp^3 , $109^\circ 28'$; p^3 , 90°) and thus the molecule should be driven further away from planar as the total ligand electronegativity increases.

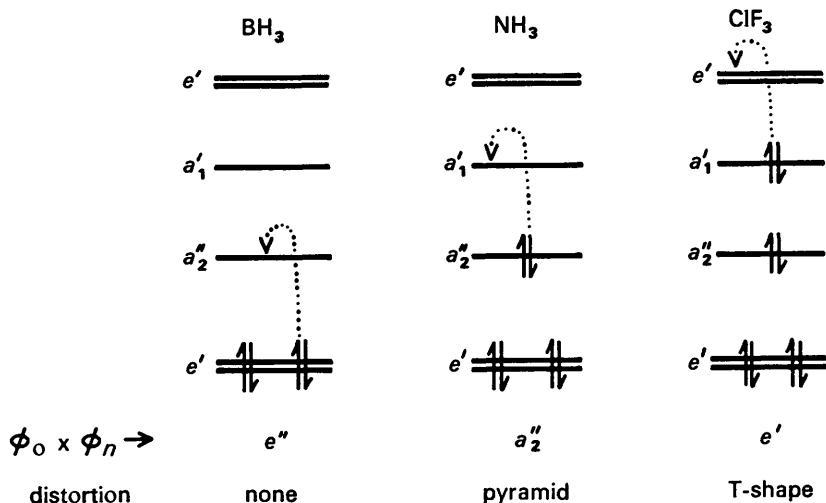
CH_3 has similar HOMO-LUMO properties to NH_3 and a distortion from the trigonal planar geometry is predicted but with a value for the relaxation term of half^{28,29} that for NH_3 (half the number of a''_2 electrons). The radical is perhaps

²¹ J. H. Current and J. K. Burdett, *J. Phys. Chem.*, 1969, **73**, 3505.

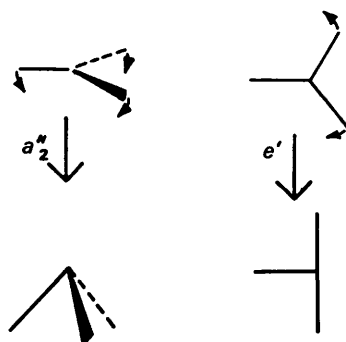
²² R. S. Mulliken, *J. Phys. Chem.*, 1937, **41**, 318; 1952, **56**, 295.

²³ J. K. Burdett, *J. Chem. Phys.*, 1970, **52**, 2983.

²⁴ J. K. Burdett, *J. Mol. Spec.*, 1970, **36**, 365.



(a)



(b)

Figure 3 (a) Second-order Jahn–Teller approach to AH_3 geometries; (b) the routes by which the a_2'' and e' bending vibrations of a trigonal planar AH_3 molecule lead to pyramidal and T-shape structures

rather tenuously planar with a vibrational frequency ($\nu_2 = 611 \text{ cm}^{-1}$) much less than in BH_3 (1125 cm^{-1}). As the ligand electronegativity increases (e.g. to CF_3) the molecules become pyramidal in accord with the ideas described above for NF_3 . By means of the fourth-order perturbation term in the expansions of equations (3) and (4) we may tackle the problem of the anharmonicity of the planar radical (and that of planar NH_3 in its first excited state). The anharmonicity may be shown²⁸ to consist of a 'classical' term and a relaxation term.

The latter is simply given by equation (6), which suggests that the larger the

$$\frac{|\langle 0 | \mathcal{H}_i | n \rangle|^2}{\Delta \epsilon} \cdot \frac{\langle n | \mathcal{H}_i | n \rangle}{(\Delta \epsilon)^2} \quad (6)$$

second-order 'softening' of the vibrational force constant, the larger the positive contribution to the quartic term in Q_i which gives rise to the negative anharmonicity. By a mechanism²⁹ which we will not discuss here the effect of perturbation by alkali halides is to reduce the relaxation term and thus increase the vibrational force constant and frequency ν_2 with a commensurate replacement of the negative anharmonicity by a normal (small) positive one (Table 1).

A molecule approachable along similar lines which also has a large second-order softening is XeF₆, a fluxional molecule in the gas phase with a large amplitude and highly anharmonic t_{1u} bending mode.³⁰ The VSEPR scheme would give the molecule (seven pairs) a much larger distortion than that actually observed.

Steric Effects.—The importance of steric effects is illustrated by a single example. For many years the pyramidal structure of N(CH₃)₃ but planar geometry of N(SiH₃)₃ has been ascribed to π -bonding between the p_z -orbital on the N atom and a Si d -orbital. However, recently Glidewell, using the ideas developed earlier by Bartell of intramolecular van der Waals forces⁶ and applied especially to hydrocarbon structures, has convincingly argued⁵ that the non-bonded repulsions of the large SiH₃ groups are large at the pyramidal geometry but are relieved at the planar. In support of this view is the fact that P(SiH₃)₃ is pyramidal. The longer P—Si bonds compared with those of N—Si result in a less tightly packed environment. N(SCF₃)₃ also has a planar NS₃ skeleton³¹ but with shortened N—S bonds, which are suggested to arise through π -bonding. The interplay between steric and electronic controls on molecular geometry is clearly an interesting one.

Summary.—The use of several different approaches leads to quite a good appreciation of the factors determining main group geometries and it is possible in some cases (*e.g.* CH₃) to understand very simply rather subtle features of the potential energy surface associated with angular deformations. We have concentrated on the geometries of covalently bound species. Structures which do not fit into the VSEPR scheme are also found for the more ionically bound members of the MX₂ series (M = Ca—Ba). In order to understand this behaviour and also some of the basic dynamics behind the operation of the Walsh diagrams, we refer the reader to a recent study by Hall.³²

3 Shapes of Transition-metal Complexes

The Failure of Existing Models.—In contrast to main group chemistry, the struc-

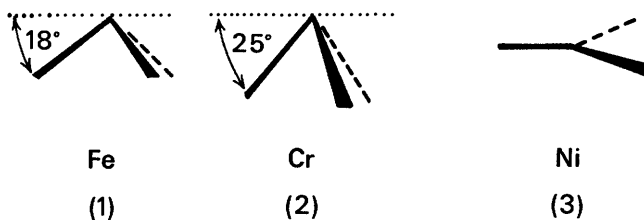
²⁹ L. S. Bartell and R. M. Gavin, *J. Chem. Phys.*, 1968, **48**, 2466.

³¹ C. J. Marsden and L. S. Bartell, *J.C.S. Dalton*, 1977, 1582.

³² M. B. Hall, *J. Amer. Chem. Soc.*, 1978, **100**, 6333; *Inorg. Chem.*, 1978, **17**, 2261.

tures of relatively few transition metal complexes are known in the gas phase. Most of the available ones are either octahedral $[\text{Cr}(\text{CO})_6, \text{MF}_6]$ or tetrahedral $(\text{VCl}_4, \text{TiCl}_4)$. The structures of complexes in crystals should be interpreted with care since the influence of the medium is not well understood, and an observed geometry in the solid may not represent the lowest energy configuration of the free molecule. It is also probably true that transition metal structures are more susceptible to distortion in the solid state so that a wider variety of structures are found. For example, CuCl_4^{2-} may adopt the D_{2d} or square planar geometry depending upon the counterion. Pressure also reversibly converts one into the other. A significant advance in the range of available transition-metal systems with a variety of co-ordination numbers and d -electron configurations was the production in low temperature matrices of binary $\text{M}(\text{CO})_n$ and $\text{M}(\text{N}_2)_n$ complexes.³³ Most of the quantitative structural determinations on these molecules have been performed in laboratories in Newcastle upon Tyne and Toronto. Some of this work is described by Poliakoff in the next article (see p. 527). The matrix does not seem to exert a strong force influencing the geometry of the molecule, and in many ways we may regard them as being pseudo gas-phase structures.

$\text{Fe}(\text{CO})_3$ (1) and $\text{Cr}(\text{CO})_3$ (2) are both pyramidal molecules with bond angles determined using the band intensity method. They were both made by the careful matrix photolysis of the parent molecules $\text{Fe}(\text{CO})_5$ ³⁴ and $\text{Cr}(\text{CO})_6$.³⁵ $\text{Ni}(\text{CO})_3$ (3) is a trigonal planar molecule.³⁶ $\text{Fe}(\text{CO})_3$ is probably a triplet species



[magnetic circular dichroism studies on $\text{Fe}(\text{CO})_4$ (see p. 531) show it to have $S = 1$] and we shall refer to its electronic configuration as $hs\ d^8$ ($hs = \text{high spin}$); $\text{Cr}(\text{CO})_3$ is certainly $ls\ d^6$ ($ls = \text{low spin}$). With three ligand σ pairs the molecules $\text{Cr}(\text{CO})_3$, $\text{Fe}(\text{CO})_3$, and $\text{Ni}(\text{CO})_3$ have a total of six, seven, and eight pairs surrounding the central atom, respectively. It is possible to find VSEPR polyhedra to rationalize their shapes (octahedron for six pairs, C_{3v} capped octahedron for seven pairs, and distorted square antiprism for eight pairs) but these polyhedra may not be used to rationalize other transition-metal structures; $\text{Cr}(\text{CO})_5$ also with eight pairs is a square pyramid³⁷ which does not fit into the square anti-

³³ J. K. Burdett, *Coord. Chem. Rev.*, 1978, **27**, 1.

³⁴ M. Poliakoff, *J.C.S. Dalton.*, 1974, 210.

³⁵ R. N. Perutz and J. J. Turner, *J. Amer. Chem. Soc.*, 1975, **97**, 4800.

³⁶ R. L. DeKock, *Inorg. Chem.*, 1971, **10**, 1205.

³⁷ R. N. Perutz and J. J. Turner, *Inorg. Chem.*, 1975, **14**, 262.

prism concept. Gillespie¹ suggested that with these carbonyls the *d*-electrons should be neglected and just the number of ligand σ pairs included. Although this correctly predicts $\text{Cr}(\text{CO})_6$ to be octahedral and $\text{Ni}(\text{CO})_4$ to be tetrahedral, all three tricarbonyls should be trigonal planar according to this model, which is not the case. The Jahn–Teller theorem may often be used to rationalize the observed geometries of transition metal complexes, although as a predictor of molecular shape it is usually not very specific. One area where this approach fails is for those cases where a distorted geometry is found but the highest symmetry structure is not orbitally degenerate and therefore is Jahn–Teller stable. Examples of this type are found in both $\text{Cr}(\text{CO})_3$ and $\text{Fe}(\text{CO})_3$.

For application of Jahn–Teller arguments we need a MO diagram for the D_{3h} structure. Two extended Hückel calculations^{38,39} have derived slightly different results as to the order of the energy levels in the trigonal planar structure [Figures 4(a) and 4(b)]. We note that both a *ls* d^6 and *hs* d^8 system on the scheme of Figure 4(a) would be Jahn–Teller unstable, but distortion to a T-shape (not to a pyramid) is predicted on group theoretical arguments.²⁵ On the scheme of Figure 4(b) both molecules would be Jahn–Teller stable. On both schemes a pyramidal (C_{3v}) geometry is unlikely for the low spin d^8 $\text{Fe}(\text{CO})_3$ molecule since here it would be Jahn–Teller unstable. On either scheme the $\text{Cr}(\text{CO})_3$ and $\text{Fe}(\text{CO})_3$ molecules are predicted to be unstable on second-order Jahn–Teller grounds. The distortion co-ordinate is of species e' which predicts a distortion to a T-shape, which is patently not the case. The higher energy transition $e'' \rightarrow e'$ does give rise to a transition density of species a''_2 for the Cr and Fe examples but the rule discussed in Section 2, p. 508 required that the lowest energy transition was most important. Here the structural predictions of the second-order Jahn–Teller effect are not reliable. This does not mean, of course, that the perturbation approach to the analysis of MO energy changes on distortion is in general invalid. It does mean, however, that the energy changes associated with a *group* of valence orbitals on distortion must be considered rather than that associated with one orbital in particular. For $\text{Ni}(\text{CO})_3$ the $e'' \rightarrow e'$ transition is not allowed since the *d* manifold is full (d^{10}).

Figure 4 also shows some quantitative calculations of the orbital energy changes on distortion. We can readily see that double occupation of the a'_1 orbital in both *ls* d^6 and *hs* d^8 molecules strongly encourages pyramidalization. The smaller distortion for $\text{Fe}(\text{CO})_3$ away from the trigonal planar geometry compared with that for $\text{Cr}(\text{CO})_3$ is simply understood since here there is double occupation of the e' orbital which is destabilized on distortion. In $\text{Ni}(\text{CO})_3$, four electrons in this orbital ensure planarity. Figure 4(c) shows that distortion to a T-shape from the trigonal plane is also favoured for the electronic configurations *ls* d^6 , *hs* d^8 . Do we need then to rely on quantitative calculations in order to predict molecular geometry? The most comprehensive sets of calculations on these angular geometries have used the extended Hückel method. In general these reproduce the observed geometries with remarkable fidelity. Both sets of

³⁸ J. K. Burdett, *J.C.S. Faraday II*, 1974, **70**, 1599.

³⁹ M. Elian and R. Hoffmann, *Inorg. Chem.*, 1975, **14**, 1058.

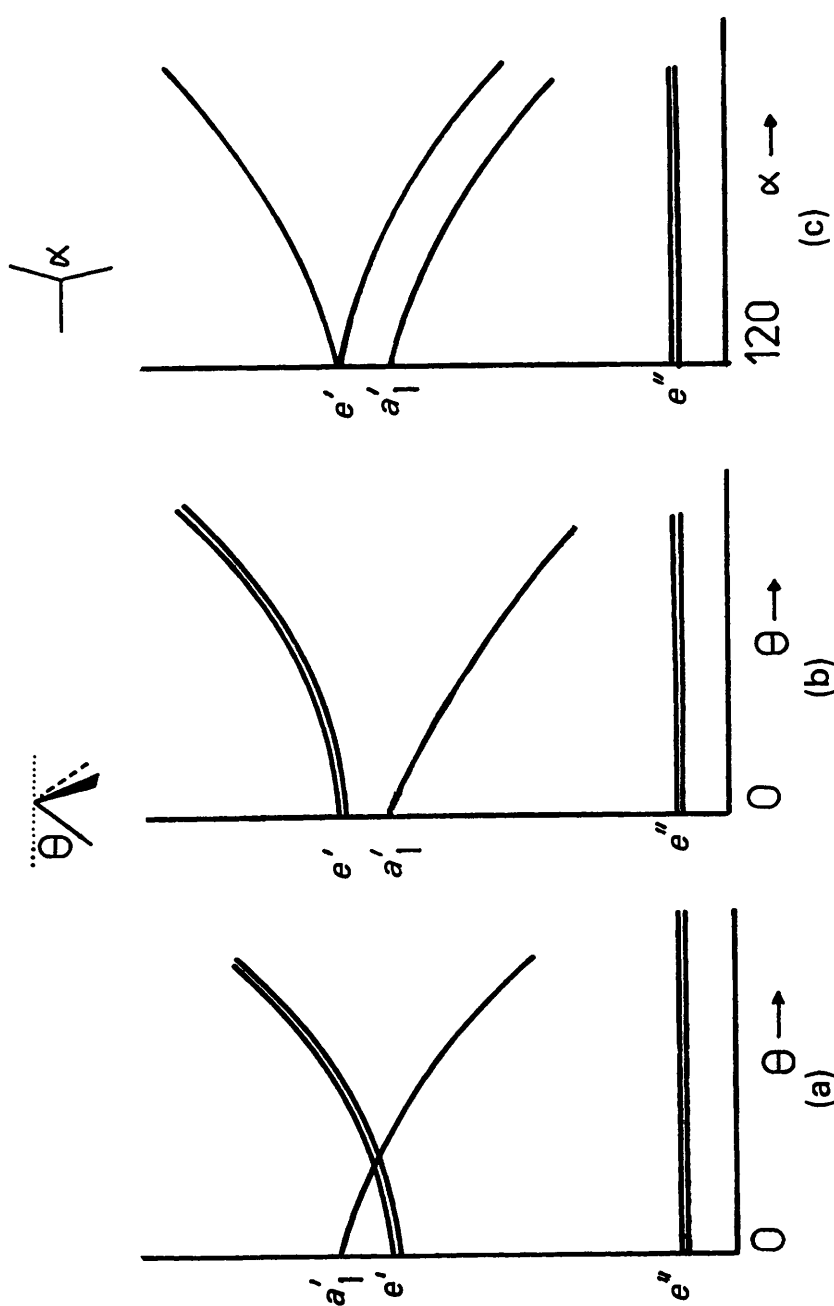


Figure 4 MO energy level diagrams for bending within; (a) C_{3v} co-ordinate, from ref. 39; (b) C_{3v} co-ordinate, from ref. 38; (c) C_{2v} co-ordinate, from ref. 38

calculations predict a D_{2d} geometry for the d^9 $M(\text{CO})_4$ species but with a C_{3v} geometry close in energy. Both forms have been made in low temperature matrices. Similarly although (hs d^8) $\text{Fe}(\text{CO})_4$ is predicted and observed to have a C_{2v} structure, a C_{3v} or C_s geometry lies close in energy above it. As described in the following article, laser i.r. photolysis experiments confirm a thermal rearrangement pathway *via* a transition state of this symmetry. For the tricarbonyl series θ is predicted to be: 30° , 33° , [obs. 25° for $\text{Mo}(\text{CO})_3$]; 17° , —, [obs. 18° in $\text{Fe}(\text{CO})_3$]; 0 , 8° , [obs. 0° in $\text{Ni}(\text{CO})_3$] from the two sets of calculations described in refs. 38 and 39, respectively.

There is clearly a need for a simple model with which to view these structures.

The Angular Overlap Approach.—Our simple molecular orbital approach is based on the angular overlap model (AOM),^{40–42} which has been used mostly in the past in the interpretation of the electronic spectra and magnetic properties of transition-metal complexes. Basically it provides the energies of the (mainly) transition metal d orbitals in an ML_n complex of given geometry in terms of two parameters, one describing σ - and the other π -type interactions. [Similar to the Δ or Dq of the crystal field theory (CFT).] Once these energies have been obtained then the weighted sum of the d -orbital energies (weighted by the number of electrons in these orbitals) as a function of the molecular geometry provides the opportunity to explore the configurational potential surface and find the most stable geometry demanded by metal d -ligand interactions for a particular electronic configuration. The AOM is based on an approximation involving the interaction energy between two orbitals (ϕ_i , ϕ_j) on different atoms. Here ϕ_i represents a metal d -orbital and ϕ_j a single ligand orbital or symmetry-adapted combination.

The stabilization energy ϵ of the bonding component may be written as a perturbation sum [equation (7)] where k is a constant, S_{ij} is the overlap integral

$$\epsilon = \frac{k^2 S_{ij}^2}{\Delta\epsilon_{ij}} - \frac{k^4 S_{ij}^4}{(\Delta\epsilon_{ij})^3} + \dots \quad (7)$$

between ϕ_i and ϕ_j , and $\Delta\epsilon_{ij}$ their unperturbed energy separation. In the following discussion we shall concentrate on the leading term in the expansion with an occasional reference to the others. The stabilization of the bonding combination becomes $\epsilon = \beta_\lambda S_{ij}^2$, where β_λ is $k^2/\Delta\epsilon_{ij}$ ($\lambda = \sigma, \pi, \text{etc.}$). In our simple model it is also assumed that the destabilization energy of the antibonding orbital is equal to the stabilization energy of its bonding partner. The tremendous power of the model lies in the fact that the S_{ij} are, in general, dependant on simple geometric expressions as the angular metal–ligand geometry is adjusted while maintaining the same bond length. This means that the following calculations may be simply performed using ‘back-of-envelope’ computations. Table 2 gives functions for overlap of a ligand σ orbital (located at the polar position θ, ϕ) with the d -orbitals,

⁴⁰ J. K. Burdett, *Adv. Inorg. Chem. Radiochem.*, 1978, **21**, 113.

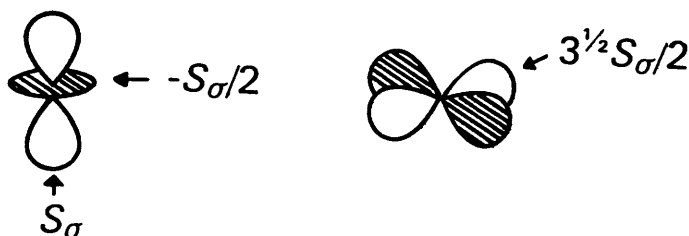
⁴¹ C. E. Schaffer and C. K. Jørgensen, *Mol. Phys.*, 1965, **9**, 401.

⁴² C. E. Schaffer, *Struct. Bonding*, 1973, **14**, 69.

Table 2 Angular dependence of ligand σ -metal d -orbital overlap integral as a function of the polar co-ordinates of the ligand

d -orbital	S
z^2	$\frac{1}{2}(3H^2 - 1)S_\sigma$
$x^2 - y^2$	$\frac{3^\pm}{2}(F^2 - G^2)S_\sigma$
xz	$3^\pm FHS_\sigma$
yz	$3^\pm GHS_\sigma$
xy	$3^\pm FGS_\sigma$

$$F = \sin\theta\cos\phi, G = \sin\theta\sin\phi, H = \cos\theta$$



and shows some of the overlap integrals which are particularly useful. Thus the interaction energy of a ligand σ orbital with the z^2 orbital is given by the function

$$\epsilon = \beta_\sigma S_\sigma^2 \frac{1}{4} (3\cos^2\theta - 1)^2, \text{ where } \beta_\sigma \text{ is introduced as the proportionality}$$

constant describing σ -type interactions. The notation used is that of Kettle;⁴³ a simpler way of expressing these values is to put $\beta_\sigma S_\sigma^2 = e_\sigma$, see for example ref. 41. π -Type interactions are described by analogous equations but we will concentrate on σ -type interactions in our discussion since these are generally considered to be of large magnitude. We are thus in a position to be able to write the interaction energy of a pair of orbitals as $\epsilon = h\beta_\sigma S_\sigma^2$, where h is a calculable number and the product $\beta_\sigma S_\sigma^2$ the AOM parameter. One way of evaluating the interaction energy is to write down a symmetry-adapted ligand σ combination and calculate its overlap integral S_{ij} with the relevant d -orbital. A quicker method of calculation for an ML_n complex is to use the ligand additivity [equation (8)] over all n ligands co-ordinated to the central metal atom. The total

$$\epsilon_t = \beta_\sigma \sum_{j=1}^n S_{ij}^2 \quad (8)$$

σ stabilization energy $\sum(\sigma)$ is then very simply given by equation (9), where h_t is the number of electron holes in the i th d -orbital. Equation (9) arises simply because

⁴³ S. F. A. Kettle, *J. Chem. Soc. (A)*, 1966, 420.

$$\Sigma(\sigma) = \Sigma h_i \epsilon_i \quad (9)$$

when filling d -orbitals with electrons we are filling metal–ligand antibonding orbitals. It is only the empty d -orbitals that have filled metal–ligand bonding counterparts which contribute to the stabilization energy.^{44,45} An interesting sum rule [equation (10)] applies to the orbital energies derived from equation (8),

$$\Sigma_i \epsilon_i = n \beta_{\sigma} S \sigma^2 \quad (10)$$

where n is the number of σ orbitals (ligands) surrounding the central atom. This can be used to check the arithmetic involved in evaluating orbital interaction energies. An exactly analogous prescription applies to the evaluation of π -bonding interactions. Care must be taken here to distinguish between π -donors (the mainly ligand located components are ML bonding but the mainly metal d -orbitals are ML antibonding) and π acceptors (the mainly metal d -located orbitals are ML bonding and the mainly ligand-located orbitals, which are usually empty, ML antibonding). The d -orbitals are destabilized in the former but stabilized in the latter case.

The AOM is then much easier to apply than the crystal field method, especially in lower symmetry environments. The CFT also differs from the drawback that σ , π bonding, which are vital concepts in modern inorganic chemistry, cannot be included in the model. Another problem with the CFT is that in lower than cubic environments two parameters, Dq and Cp are needed to describe the energy levels. The two are related *via* a parameter ρ . In most places where the CFT is used in low symmetry situations a value of $\rho = 1$ is arbitrarily used.⁴⁶ From spectroscopic measurements larger values are probably more accurate but the factors governing the exact choice of ρ in different environments is far from clear.

Figure 5 shows the d -orbital energy levels of geometries of interest obtained from simple calculations involving the overlap integrals. (A slight complication occurs in the T-shape geometry where two d -orbitals have the same symmetry, and allowance for mixing of these orbitals needs to be made.⁴⁷)

Geometries of Complexes.—We have shown elsewhere that the variation in the heats of hydration of the M^{2+} ions across the first row transition-metal series, one of the classic successes of the CFT, is similarly described by our molecular orbital model.⁴⁶ The forces contributing to $\Delta H^{\circ}_{\text{hyd}}$ are the metal nd -ligand interaction augmented by contributions from ligand interactions with metal $(n + 1)$ s, p -orbitals. These observations suggest that the observed angular geometry will be a balance between that demanded by s, p interactions and that by the d -orbital interactions with the ligands. In general an ML_n complex contains $n\sigma$ pairs of electrons which are involved in s, p (and d) interactions.

⁴⁴ J. K. Burdett, *Inorg. Chem.*, 1975, **14**, 375.

⁴⁵ J. K. Burdett, *Inorg. Chem.*, 1976, **15**, 212.

⁴⁶ J. K. Burdett, *J.C.S. Dalton*, 1976, 1725.

⁴⁷ D. S. McClure, in 'Advances in the Chemistry of the Coordination Compounds', ed. S. Kirschner, Macmillan, New York, 1961, p. 498.

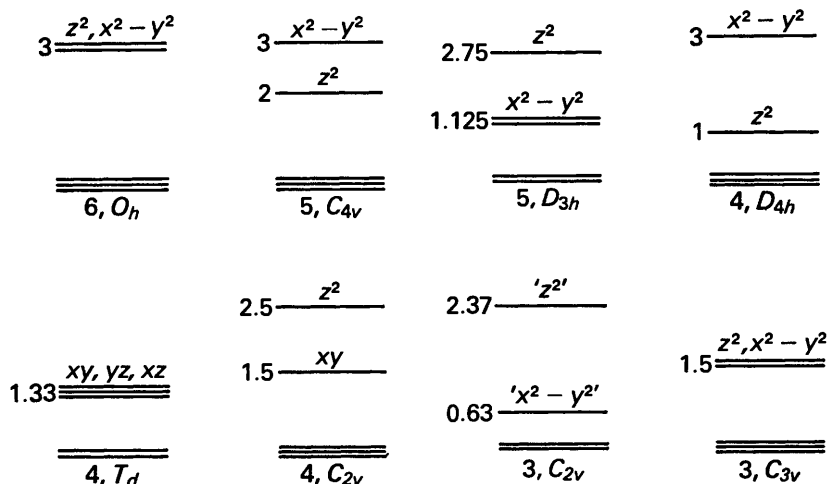


Figure 5 MO diagrams in the d -orbital region for some geometries of interest (energy units $\beta_{\sigma}S_{\sigma}^2$ or e_{σ}). The co-ordination number and molecular point group are given under each diagram. In the geometries with an angular degree of freedom (e.g. 4, C_{2v}) the n ligands are placed at the vertices of an octahedron such that LML angles are either 90° or 180°

Using the VSEPR method (which often dealt successfully with the shapes of molecules with s, p -orbitals alone on the central atom) the geometry demanded by interactions with these higher orbitals will be trigonal planar (D_{3h}) for ML_3 and tetrahedral (T_d) for ML_4 etc. We note that in these molecules the VSEPR geometry is the one with minimum ligand pair repulsions (Pauli avoidance) and also the one containing minimum non-bonded repulsions between the ligands themselves. We call these combined forces, ligand-ligand terms.

From Figure 5 we can readily calculate the d -orbital stabilization energy for the various three-co-ordinate geometries which we include here as a function of d -electron configuration. For $1s d^8$, $1s d^8$, $hs d^8$, and d^{10} the results are given in Table 3. There is of course no d -orbital stabilization for $Ni(CO)_3$ at any geometry since all bonding and antibonding orbitals are filled. For the two other molecules the T-shape and 'octahedral *fac* trivacant' (C_{3v} pyramid) geometries have the same d -orbital energy. We need to turn to the fourth-order term in equation (7) to resolve them. The general result is that the structure with the largest number of *cis* ligands is more stable. (If the ligands are π acceptors, π stabilization is also maximized at this geometry.) The driving force away from the D_{3h} geometry is larger for $Cr(CO)_3$ ($1.5\beta_{\sigma}S_{\sigma}^2$) than for $Fe(CO)_3$ ($0.75\beta_{\sigma}S_{\sigma}^2$). $Cr(CO)_3$ has the structure which is most distorted ($\theta = 25^\circ$) from trigonal planar. $Ni(CO)_3$

Table 3 *d*-Orbital stabilization energies for some three-co-ordinate structures (units $\beta_{\sigma}S_{\sigma}^2$ or e_{σ})

<i>d</i> -electron configuration ^a	C_{3v}^b	D_{3h}	C_{2v}^c	example
ls d^6 (22200)	6.0	4.5	6.0	Cr(CO) ₃
ls d^8 (22220)	3.0	2.25	4.73	Rh(P Ph ₃) ₃ ⁺
hs d^8 (22211)	3.0	2.25	3.0	Fe(CO) ₃
d^9 (22221)	1.5	1.125	2.37	
d^{10} (22222)	0	0	0	Ni(CO) ₃

^a*d*-Orbital occupation numbers in parentheses, lowest energy orbital first; ^bLML angles 90° (octahedral *fac* 'trivacant'); ^cLML angles 90°, 180° (T-shape)

has no driving force away from the D_{3h} geometry and thus remains planar, held there by ligand–ligand forces. Recently the T-shaped structure predicted for the three-co-ordinate ls d^8 ML₃ system has been observed⁴⁸ in a crystallographic environment for Rh(PPh₃)₃⁺. All the observed geometries are in encouraging agreement with those predicted. Of course all we have done really is to calculate, using a simple model, the relative energies of the e and a_1 orbitals shown in Figures 4(a) and (b) compared with those of the orbitals of Figure 4(c).

Similar arguments may be used to understand the geometries of four-co-ordinate molecules,⁴⁴ using Table 4. Cr(CO)₄ with a larger driving force away

Table 4 *d*-Orbital stabilization energies for some four-co-ordinate structures (units $\beta_{\sigma}S_{\sigma}^2$ or e_{σ})

<i>d</i> -electron configuration	D_{4h}	T_d	C_{2v}^a	example
ls d^6 (22200)	8.0	5.3	8.0	Cr(CO) ₄
ls d^8 (22220)	6.0	2.67	5.0	Ni(CN) ₄ ²⁻
hs d^8 (22211)	4.0	2.67	5.0	Fe(CO) ₄
d^9 (22221)	3.0	1.33	2.5	CuCl ₄ ²⁻
d^{10} (22222)	0	0	0	Ni(CO) ₄

^aLML angles 90°, 180° (octahedral *cis* 'divacant')

from tetrahedral than Fe(CO)₄ gives the more distorted geometry [the *cis*-divacant is more stable than the square planar for this configuration by considering the fourth-order terms of equation (7)]. Ni(CN)₄²⁻ is found as the square planar molecule but the d^9 system CuCl₄²⁻ has a smaller driving force from tetra-

⁴⁸ Y. W. Yared, S. L. Miles, R. Bau, and C. A. Reed, *J. Amer. Chem. Soc.*, 1977, **99**, 7076.

hedral and is sometimes found in square planar and sometimes in D_{2d} environments⁴⁹ (Figure 6). The reluctance of the $1s d^8$ square planar geometry to add

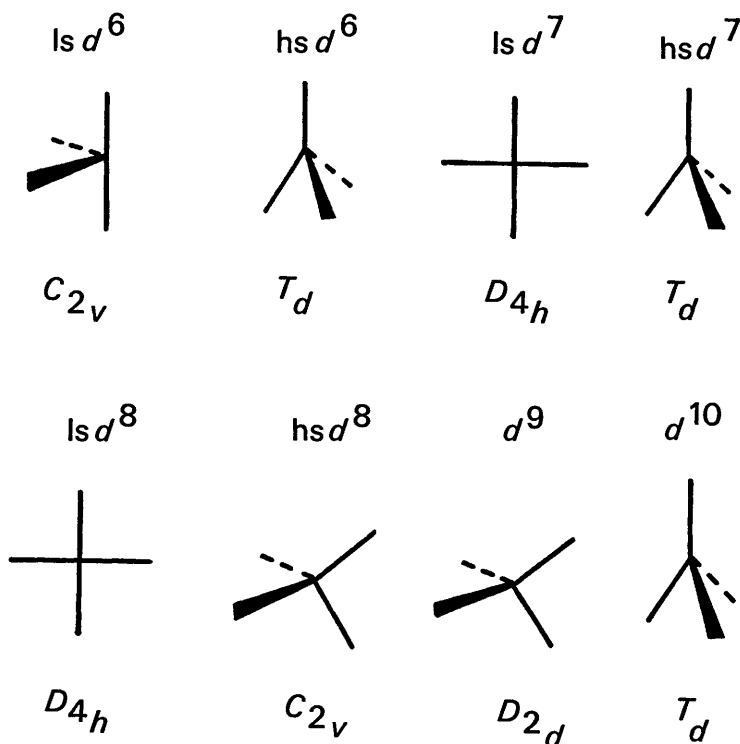


Figure 6 Observed geometries of four co-ordinate molecules as a function of d -electron configuration. Examples: d^6 , $\text{Cr}(\text{CO})_4$ ($1s$), FeCl_4^{2-} (hs); d^7 $\text{Rh}\{\text{S}_2\text{C}_2(\text{CN})_2\}_2^{2-}$ ($1s$), CoCl_4^{2-} (hs); d^8 $\text{Ni}(\text{CN})_4^{2-}$ ($1s$), $\text{Fe}(\text{CO})_4$ (hs); d^9 CuCl_4^{2-} (a variety of geometries are found for this electronic configuration); d^{10} $\text{Ni}(\text{CO})_4$

two more ligands to complete an octahedron is another structural feature of these molecules that we can view using our method.⁵⁰ In addition the kinetic behaviour of ligand substitution in this system (*trans* effect) is another field where this simple parametrized model is successful.⁵¹

For five-co-ordinate molecules, ground state $\text{Cr}(\text{CO})_5$ ($1s d^6$) has the largest stabilization energy for the square pyramid compared with trigonal bipyramid geometry. $\text{Fe}(\text{CO})_5$ with only a small distortion energy is found as the trigonal bipyramid although it is fluxional, probably *via* a square pyramid transition state. The trigonal bipyramid is predicted for the first excited state of $\text{Cr}(\text{CO})_5$

⁴⁹ J. R. Ferraro and J. Long, *Accounts Chem. Res.*, 1975, 8, 171.

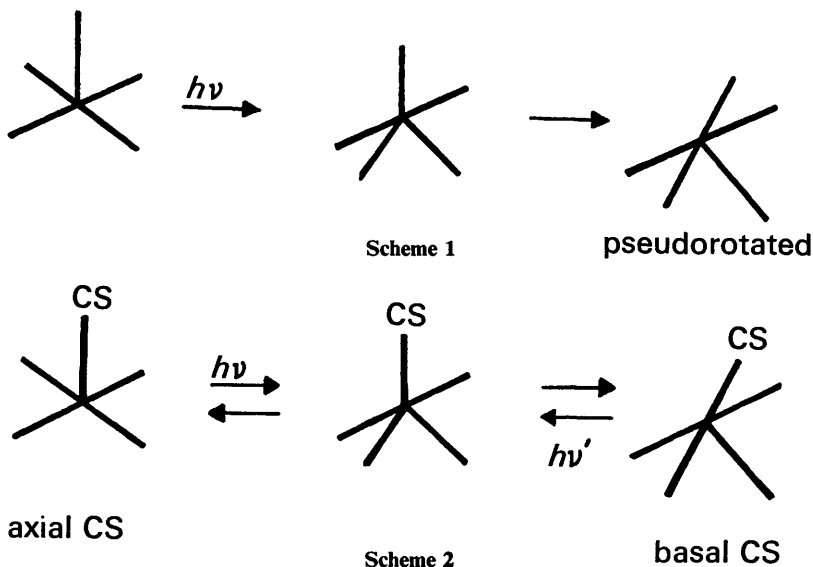
⁵⁰ J. K. Burdett, *Inorg. Chem.*, 1975, 14, 931.

⁵¹ J. K. Burdett, *Inorg. Chem.*, 1977, 16, 3013.

Table 5 *d*-Orbital stabilization energies for some five-co-ordinate structures (units $\beta_{\sigma}S_{\sigma}^2$ or e_{σ})

<i>d</i> -electron configuration	C_{4v}	D_{3h}	difference	example
1s d^6 (22200)	10.0	7.75	2.75	Cr(CO) ₅
1s d^6 (22110)	8.0	7.75	0.25	Cr(CO) ₅ *
1s d^7 (22210)	8.0	6.625	1.375	Mn(CO) ₅
1s d^8 (22220)	6.0	5.5	0.5	Fe(CO) ₅

since the driving force away from this geometry is smaller than for Fe(CO)₅. Matrix experiments with this molecule using polarized spectroscopy and photolysis, Scheme 1,⁵² and visible photolysis studies on Cr(CO)₄CS, Scheme 2⁵³ show that this is very probable.



Thus the idea of a balance between VSEPR steric and *d*-orbital demands in controlling the shape of the molecule is a very satisfying one. A general observation is that the larger the *d*-orbital driving force away from the ligand–ligand determined geometry the closer the observed geometry is to the *d*-orbital only prediction. Thus Ni(CN)₄²⁻ (driving force = 3.3 $\beta_{\sigma}S_{\sigma}^2$) is a regular square plane, Cr(CO)₄ (2.25 $\beta_{\sigma}S_{\sigma}^2$) and Cr(CO)₅ (2.33 $\beta_{\sigma}S_{\sigma}^2$) have bond angles close to 90°

⁵² J. K. Burdett, J. M. Grzybowski, R. N. Perutz, M. Poliakoff, J. J. Turner, and R. F. Turner, *Inorg. Chem.*, 1978, 17, 147.

⁵³ M. Poliakoff, *Inorg. Chem.*, 1976, 15, 2022, 2892.

and 180° but $\text{Cr}(\text{CO})_3$ ($1.5 \beta_\sigma S_\sigma^2$) is less than two thirds the way to the *fac* octahedral trivacant structure.

Steric Effects.—Table 6 shows the result of calculations designed to reveal the relative stability of a series of eight-co-ordinate geometries.⁵⁴ Extended Hückel

Table 6

<i>geometry</i>	<i>electronic stabilization^a energy from AOM of d^0 ML_8</i>	<i>steric energy EHMO results on L_8^{8-} /kcal mol⁻¹</i>
dodecahedron	77.2	3.5
square antiprism	76.4	0 ^b
square prism (cube)	85.2	27
hexagonal bipyramid	86.8	97
C_{3v} bicapped trigonal prism	71.4	166
C_{2v} bicapped trigonal prism	75.2	24

^aunits are $k^4 S_\sigma^4 (\Delta\epsilon_{ij})^{-3} = \gamma_\sigma S_\sigma^4$ from equation (7); ^b*i.e.* on steric grounds the square antiprism is the most stable geometry

calculations on the L_8^{8-} system itself (ML_8 but without the metal atom) gave the relative steric (a contributor to the ligand–ligand terms above) merits of the various structures. Evaluation of the fourth-order terms of equation (7) gave the electronic advantages for each geometry [since these are included with a minus sign in equation (7) the smaller this contribution the more favourable the structure]. From the sum rule of equation (10) the second-order terms are equal for all geometries if we assume d^0 configurations. The superposition of the two series gives a good description of the popularity of the various structures. There are a large number of dodecahedral and square antiprismatic structures—good on both steric and electronic grounds. An increasing number of C_{2v} BTP geometries are being identified as a result of the use of various crystallographic shape parameters. These geometries and intermediate versions make up the vast majority of eight-co-ordinate examples. The cube and hexagonal bipyramid are not very good on either basis; only three examples of the former are known and a handful of hexagonal bipyramid structures if the special case of UO_2 containing systems is excluded. The D_{3h} bicapped trigonal prism is a combination of excellent electronic but very poor steric stability. There are no characterized examples with transition metal ions. Steric effects are therefore clearly important in the geometry field, especially with the higher co-ordination numbers, and may often work against electronic factors. The molecular mechanics results of Kepert⁵⁵ and the existence of small co-ordination number molecules with bulky

⁵⁴ J. K. Burdett, R. C. Fay, and R. Hoffmann, *Inorg. Chem.*, 1978, 17, 2553.

⁵⁵ D. L. Kepert, *Progr. Inorg. Chem.*, 1977, 23, 1.

ligands as demonstrated by Bradley⁵⁶ also strikingly reveal the importance of these non-bonded effects.

Finally we must also mention here Johnson's intriguing method⁵⁷ for determining the stereochemistry of $M_n(CO)_m$ species, the elucidation of the number and position of terminal, doubly, and triply bridging carbonyl groups, and the geometry of the metal skeleton. The spatial arrangement of the CO groups is found to be one of the close packed arrangements of m spheres. The metal atoms are located at positions set by the best arrangement of an M_n polyhedron within this structure. The resulting geometrical relationships between each M and a given CO determine whether the latter is in a terminal, doubly, or triply bridging position. This essentially steric argument is the first theoretical method which is able to predict polynuclear carbonyl stereochemistry with any success. It remains to be seen if a MO alternative can be developed.

I would like to thank my friends and colleagues who, over the years, have provided a stimulating environment in which to work, especially J. J. Turner and M. Poliakoff for a period of particularly exciting interaction in which many new ideas were conceived.

⁵⁶ D. C. Bradley, *Chem. in Britain*, 1975, **11**, 393; P. G. Eller, D. C. Bradley, M. B. Hursthouse, and D. W. Meek, *Coord. Chem. Rev.*, 1977, **24**, 1.

⁵⁷ B. F. G. Johnson, *Chem. Comm.*, 1976, 211.